



Numerical analysis of the wall impact in the peristaltic pumping of a casson liquid in an inclined canal

Ramu Katipelli^{a,*}, SHVN Krishna Kumari^b

^aAssistant Professor, Department of Science and Humanities, Siddhartha Institute of Technology and Sciences, Narapally, Hyderabad-500088, Telangana.

^bProfessor, Department of Mathematics, Koneru Lakshmaiah Education Foundation, R.V.S Nagar, Aziznagar Telangana-500075.

(Communicated by Madjid Eshaghi Gordji)

Abstract

Flow is considered in the moving frame of reference with constant velocity along the wave. The developed mathematical model is presented by a set of partial differential equations. A numerical algorithm based on finite element method is implemented to evaluate the numerical solution of the governing partial differential equations in the stream-vorticity formulation. This paper is about the study of Numerical analysis of the peristaltic conveyance of a casson fluid in a skewed tube under the consideration of low Reynolds and long wavelength. The problem is discussed on the inclination angle and yield stress of a fluid are examined for different qualitative and quantitative effects on pressure and also the trapping bolus creation analyzed by changing various parameters, the equation of flux analyzed in a wave frame moving at wave speed. Expressions are derived for the frictional force, change in volume flow rate, rise and drop in pressure. The impact of frictional force on various parameters on the pumping characteristics and pressure flow curves discussed through graphs.

Keywords: Peristaltic pumping, Casson fluid, inclined channel, Non-Newtonian fluid, trapping, frictional force.

*Corresponding author

Email addresses: katipellir@gmail.com (Ramu Katipelli), krishnagannamaraju@gmail.com (SHVN Krishna Kumari)

1. Introduction

The transfer of peristalsis is an extension and a contraction of an extending fluid tube induced by a constant surface contraction wave Sarkar B.C et al. [15]. The physicists know that the peristalsis is one of the main processes in many biological processes for the transfer of fluids. Bhatti M.M., Ellahi R et al. and Ijaz N et al. [3, 10]. The operation of the ureter, food-and-chyme-motion mixing in the stomach, ovarian motion in the fallopian tube, sperm transfer to the cervical canal, transfer of cilia and blood flow in the arteries of the blood are usually apparent Akbar et al. [2]. For industrial uses, such as hygienic fluid transmission, heart lung blood pumps and corrosive liquid transportation for which fluid interaction with the mechanical components is forbidden, a peristaltic transport mechanism has been utilized Ellahi et al. [7]. Blood and other physiological fluids have been taken as Newtonian fluid in most compute physics. This strategy, even though it can provide a model appropriate of the ureter's peristaltic process KrishnaKumari et al. [11], does not offer a satisfactory model for small blood vessels and lymphatic vessels, intestines, efferentes in male reproductive transport and transport of the spermatogenesis Gnaneswara Reddy et al. and Vajravelu et al. [14, 16] to the cervical canal when the peristaltic technique has a negative impact. Most physiologic liquids have now been recognized to be non-Newtonian Mekheimer et al. and Vajravelu et al. [12, 9].

2. Review of Literature

Sarkar et.al [15] discussed the numerical result on hydro magnetic nanomagnetic peristaltic movement in the asymmetric channel for the effect of thermal radiation and forces acting. While the existence of surface lubricants through micro channels or tiny capillaries in peristaltic fluid motion leads to a speed shift, and hence no slip conditions for this type of flux cannot be used.

Bhatti et.al [3] have studied the impact of the embedded solid particles on the hydrate magnetic movement and thermal expansion of Ree-Eyring fluid into a channel was investigated using the varied features and circumstances. Peristalsis magnetic field produced their results showed a decrease in the speed profiles.

Ijaz et.al [10] analyzed the influence of nanoparticles on non-Newtonian hydro magnetic flow and analysis for the Jeffrey fluid peristaltic flow in the slip asymmetrical tilt channel. The mathematical models are theoretically determined and resolved.

Akbar et.al [2] to include the magnetic field, slip-speed, porous medium and uniform heat source impacts of heat transfer. Due to its broad use in the utilized sector, especially in the recovery of petroleum oil and syrup medicines as well as in the manufacturing of plastic goods, the study on Non-Newtonian fluids has received greater interest. Casson's fluid is one of the distinctive non-Newtonian fluids and was established by Casson in the development of its rheological model.

Agrawalet. al [1] discussed the impact of a magnetic field externally applied on the peristaltic fluid-conducting movement of a stenosed channel evenly branching. Their results indicate that the magnetic field is suitable for cardiac procedures.

Hariharan et.al, [8] discussed the Non-Newtonian fluid peristaltic transfer into a different waveform tube.

Hayat et al. [9] investigated peristaltic flow in a canal with various wave patterns and a peristaltic Jeffrey fluid channel flow with porous media supporting walls was explored. The flow in a peristaltic canal was examined.

Vajravelu et.al [16] discussed the channels and the slanted tube of a Herschel-Bulkley fluid flow. The entrapment bounds for Bingham and power law fluids have been determined. The pumping fluid is considered as non-Newtonian fluid and the influence of wall characteristics on the physiological conduit is ignored by all these studies on peristaltic flow.

S.V.H.N.KrishnaKumari.P et.al [11] was dedicated to studying the Casson fluid peristaltic motion in a slanted channel under magnetic field influence. The problem will be resolved by long wave length and low number assumptions of Reynolds. Pressure increase, volume flow rate and frictional force expressions are calculated. The influence on the theses is addressed of magnetic parameters, amplitude ratio, rendering stress, inclination angle and plugs.

3. Mathematical Formulation

We examine at the peristaltic transfer of the fluid Casson across a two-dimensional tube with a width of $2a$ and an angle β to a horizontal one [4]. We assume an indefinite wave train along the wall at speed c . We have chosen a rectangle channel X coordinative system along the centerline towards wave spread and Y orthogonal to it and assume axisymmetric channel [1]. As illustrated in figure 1 the geometry of the wall is intended to be

$$Y = S(X, t) = a + b \sin \sin \frac{2\pi}{\lambda}(X - ct) \quad (3.1)$$

where b is the amplitude of the wave and λ is the wavelength.

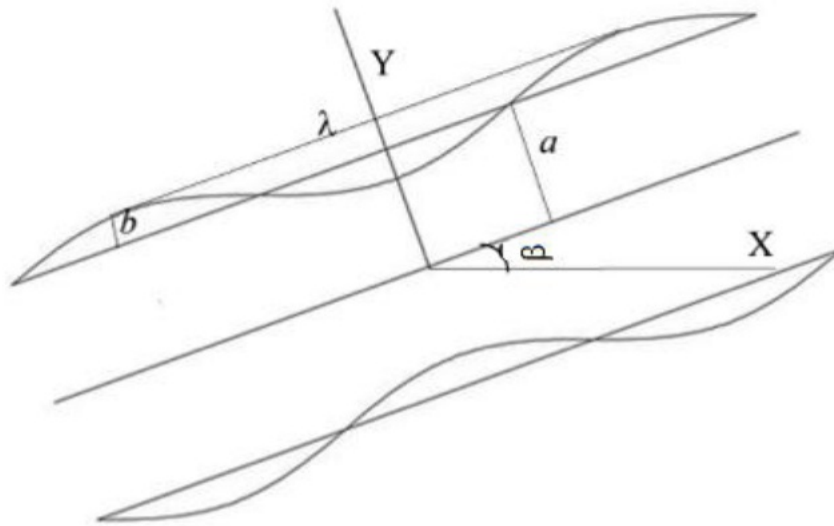


Figure 1: Schematic diagram of the inclined channel

The equations of motion are provided by assuming the infinite wavelength and the inertial components are neglected

$$\rho \frac{\partial U}{\partial t} = -\frac{\partial P}{\partial X} - \frac{\partial \varepsilon_y}{\partial Y} + \rho g \sin \sin \beta \quad (3.2)$$

$$\frac{\partial P}{\partial Y} = 0 \quad (3.3)$$

Where ρ is the density, U is the axial velocity, t is the time, P is the pressure and ε is the shear stress and g is acceleration due to gravity. The composite equation of the Casson corresponds to the flow

$$\varepsilon^{\frac{1}{2}} = \varepsilon_y^{\frac{1}{2}} + \left(-\sigma \frac{\partial U}{\partial Y} \right)^{\frac{1}{2}} \quad \text{if } \varepsilon \geq \varepsilon_y \quad (3.4)$$

and

$$\frac{\partial U}{\partial Y} = 0 \quad \text{if} \quad \varepsilon \leq \varepsilon_y \tag{3.5}$$

Where ε_y the yield stress and σ is the viscosity of the fluid. The appropriate limit criteria are specified by

$$U(Y = S) = 0 \tag{3.6}$$

$$-\varepsilon(Y = -Y_p) = \varepsilon_y = \varepsilon(Y = Y_p) \tag{3.7}$$

$$U(Y = Y_p) = U_p \tag{3.8}$$

where U_p is the plug flow velocity and Y_p is the half width of the plug flow region.

Assuming that the channel length is an integral multiple of wavelength λ and that there is a constant pressure differential between the ends of the channel, the flow in the wave frame is constant. The difference between $O(X, Y)$ standard and $o(x, y)$ moving frame is indicated.

$$x = X - ct, \quad y = Y \tag{3.9}$$

$$u(x, y) = U(X - ct, Y) - c, \quad v(x, y) = V(X - ct, Y) \tag{3.10}$$

and

$$p(x) = P(X, t) \tag{3.11}$$

The P pressure is constant throughout each axial position of the channel, perhaps because to the enormous wavelength and the negligible curvature effects [8], where the velocity parts (u, v) and (U, V) . p and P are the wave or the fixed referral frame pressures, respectively. As non-dimensional, the following equations are introduced [13]

$$\begin{aligned} \underline{x} &= \frac{x}{\lambda}, \quad \underline{y} = \frac{y}{a}, \quad \underline{u} = \frac{u}{c}, \quad \underline{v} = \frac{v}{c\delta}, \quad \delta = \frac{b}{\lambda}, \quad \underline{p} = \frac{p}{\frac{\sigma c \lambda}{a^2}}, \quad \underline{\varepsilon} = \frac{\varepsilon}{\frac{\sigma_\infty c}{a}}, \\ \underline{\varepsilon}_y &= \frac{\varepsilon_y}{\frac{\sigma_\infty c}{a}}, \quad \underline{s} = \frac{S}{a}, \quad \underline{y}_p = \frac{y_p}{a}, \quad \underline{\emptyset} = \frac{b}{a}, \quad F = \frac{\sigma c}{\rho g a^2}, \quad \underline{u}_p = \frac{u_p}{c} \end{aligned} \tag{3.12}$$

where σ_∞ is the Newtonian viscosity of the fluid. The non-dimensional wall formulas are provided after eliminating bars

$$y = s(x) = 1 + \emptyset \sin \sin(2\pi x) \tag{3.13}$$

In dimensionless form the equations of motion become

$$\frac{\partial \varepsilon}{\partial y} = -\frac{dp}{dy} + \frac{\sin \sin \beta}{F} \tag{3.14}$$

$$0 = \frac{dp}{dy} \tag{3.15}$$

The non-dimensional version of Casson's constitutive equation is

$$\frac{\partial u}{\partial y} = -\left(\varepsilon + \varepsilon_y - 2\varepsilon_y^{\frac{1}{2}}\varepsilon^{\frac{1}{2}}\right) \quad \text{if} \quad y_p \leq y \leq s(x) \tag{3.16}$$

$$\frac{\partial u}{\partial y} = 0 \quad \text{if} \quad 0 \leq y \leq y_p \tag{3.17}$$

The respective limits in non-dimensional form are

$$u(y = s) = -1 \tag{3.18}$$

$$-\varepsilon(y = -y_p) = \varepsilon_y = \varepsilon(y = y_p) \tag{3.19}$$

$$u(y = y_p) = u_p \tag{3.20}$$

The volume flow rate is determined in a fixed frame

$$N = \int_0^S U dy = \int_0^{Y_p} U_p dy + \int_{Y_p}^S U dy \tag{3.21}$$

If n is the rate of flow independent of x and t in wave frame then

$$n = \int_0^s u dy = \int_0^{y_p} u_p dy + \int_{y_p}^s u dy \tag{3.22}$$

It follows that $N = n + s$.

The average flow rate for the peristaltic wave for one period is defined as

$$T = \lambda/c \tag{3.23}$$

$$\theta = \frac{1}{T} \int_0^T N dt = n + 1. \tag{3.24}$$

4. Method of Solution

The solution of the Eq. (4.1) and (4.2) by using (4.3)

$$\varepsilon = \left[\frac{dp}{dx} + \frac{\sin \sin \beta}{F} \right] y \tag{4.1}$$

The velocity distribution expressions in different locations may be obtained by substitutions for ε from (4.1) in the Eq. (3.16) and (3.17) constitutive and integrating with the aid of boundary conditions (3.18) and (3.20), as

$$u(y) = -1 + \frac{1}{2} \left[-\frac{dp}{dx} + f \right] \left\{ (s^2 - y^2) + 2y_p(s - y) - \frac{8}{3} \sqrt{y_p} (8^{\frac{3}{2}} - y^{\frac{3}{2}}) \right\} \tag{4.2}$$

for $y_p \leq y \leq s(x)$

$$u_p = -1 + \frac{1}{2} \left[-\frac{dp}{dx} + f \right] \left\{ s^2 + 2sy_p - \frac{8}{3} s^{\frac{3}{2}} y_p^{\frac{1}{2}} - \frac{1}{3} y_p^2 \right\} \tag{4.3}$$

for $0 \leq y \leq y_p$

where

$$y_p = \frac{s_y}{-\frac{dp}{dx} + F} \quad \text{and} \quad f = -\frac{\sin \sin \beta}{F} \tag{4.4}$$

The Eq. (4.2) and (4.3) are integrated with the condition $\varphi = 0$ at $y = 0$ and also with continuity of the stream function, the stream function is given as an equation as

$$\begin{aligned} \varphi &= -y + \frac{1}{2} \left[-\frac{dp}{dx} + f \right] s^3 \\ &\left\{ \frac{y}{s} - \frac{1}{3} \left(\frac{y}{s} \right)^3 + 2\frac{y_p}{s} \left[\frac{y}{s} - \frac{1}{2} \left(\frac{y}{s} \right)^2 \right] - \frac{8}{3} \sqrt{\frac{y_p}{s}} \left[\frac{y}{s} - \frac{2}{5} \left(\frac{y}{s} \right)^{\frac{5}{2}} \right] - \frac{1}{15} \left(\frac{y_p}{s} \right)^3 \right\} \\ &\hspace{15em} \text{for } y_p \leq y \leq s(x) \\ \varphi_p &= -y + \frac{1}{2} \left[-\frac{dp}{dx} + f \right] y \left\{ s^2 + 2y_p s - \frac{8}{3} \sqrt{y_p s^{\frac{3}{2}}} - \frac{1}{3} y_p^3 \right\} \quad \text{for } 0 \leq y \leq y_p \end{aligned} \tag{4.5}$$

The gradient of pressure is achieved by applying Eq. (3.22), (4.2) and (4.3)

$$\frac{dp}{dx} = -\frac{3(n+s)}{s^3 z(X)} = f \tag{4.6}$$

Where

$$z(x) = 1 + \frac{3}{2} \left(\frac{y_p}{s} \right) - \frac{12}{5} \sqrt{\frac{y_p}{s}} - \frac{1}{10} \left(\frac{y_p}{s} \right)^3 \tag{4.7}$$

The pressure rise per wavelength is provided by

$$\Delta P = \int_0^1 \frac{dp}{dx} dx = f - 3[nK_1 + K_2] \tag{4.8}$$

Where

$$K_1 = \int_0^1 \frac{1}{s^3 z(x)} dx \tag{4.9}$$

$$K_2 = \int_0^1 \frac{1}{s^2 z(x)} dx \tag{4.10}$$

And θ can be written as

$$\theta = \frac{f - \Delta P - 3(K_2 - K_1)}{3K_1} \tag{4.11}$$

The dimension time mean flow θ_0 for zero pressure rise is given by

$$\theta_0 = \frac{f - 3(K_2 - K_1)}{3K_1} \tag{4.12}$$

Also the dimensionless pressure rise for zero time mean flow is obtained as

$$(\Delta P)_{\theta=0} = \Delta P = f - 3(K_2 - K_1) \tag{4.13}$$

The frictional force F_λ at the wall is obtained as

$$F_\lambda = \int_0^1 s \frac{dp}{dx} dx = f - 3(\theta - 1)K_2 - 3K_3 \tag{4.14}$$

Where

$$K_3 = \int_0^1 \frac{1}{sz(x)} dx \tag{4.15}$$

5. Results and Discussion

The fluctuation in dimensional pressure drop ΔP , and the trapping phenomena for the fluctuation of half plug width yp , angle of inclination β and amplitude ratio φ are observed and visually evaluated by selecting the variable F . In $yp = 0$, the findings decreased to Newtonian fluid, and in case of straight channels if $\beta = 0$ the results were reduced.

Pumping Characteristics

When the $\Delta P = 0$ pressure is referred to as the free pumping and matching average time stream is referred to as θ_0 . The pressure increases needed to generate zero time, averaged flux of ΔP_0 shown. When $\Delta P_0 < 0$, the pressure helps the flow and is referred to as co-pumping. The change in flux rate in figure 2-4 is shown to show that all curves are uniform. The change of ΔP with θ when $\beta = \pi/4, \varphi = 0.3$ can be observed from figure 2 with modification of half plug width yp interestingly, all curves in the area of free pump ($\Delta P > 0$) are intersected at $\theta = 0.15$. For $0 \leq \theta \leq 0.15$ we observed that ΔP increases with yp i.e. pumping region increases with yp and greater than the Newtonian fluid and in the rest of the region ΔP decreases with yp i.e larger the free pumping flux with larger yp .

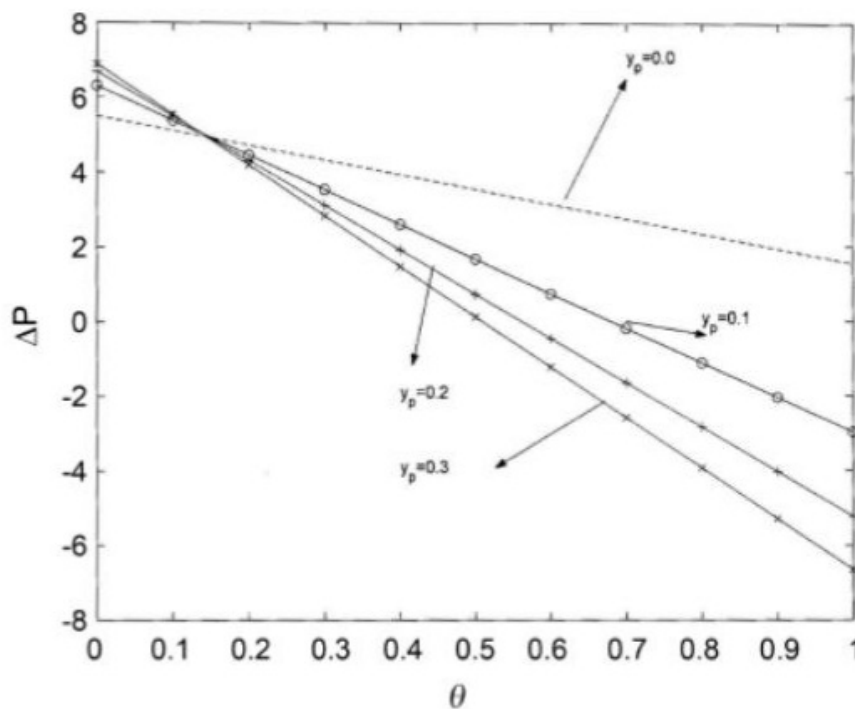


Figure 2: Variation of ΔP with θ when $F = 0.2, \beta = \pi/4, \varphi = 0.3$.

The fluctuation of a value of ΔP with θ with a value of $yp = 0.1, \varphi = 0.3$ for various values of β shown in Figure 3. It was noted that with increasing angles of inclination β , the pumping area ($0 \leq \Delta P \leq P_0$) Was increasing, with β increasing, and that for various $\beta, \Delta P = 0$ with varied $\beta = 0$, and β to take $\Delta P = 0$.

Figure 4 shows the change in the amplitude ratio of φ with ΔP with θ for $yp = 0.1, \beta = \pi/10$. The region grows and also observes that increase is greater with φ . As φ increases the pumping. The lines

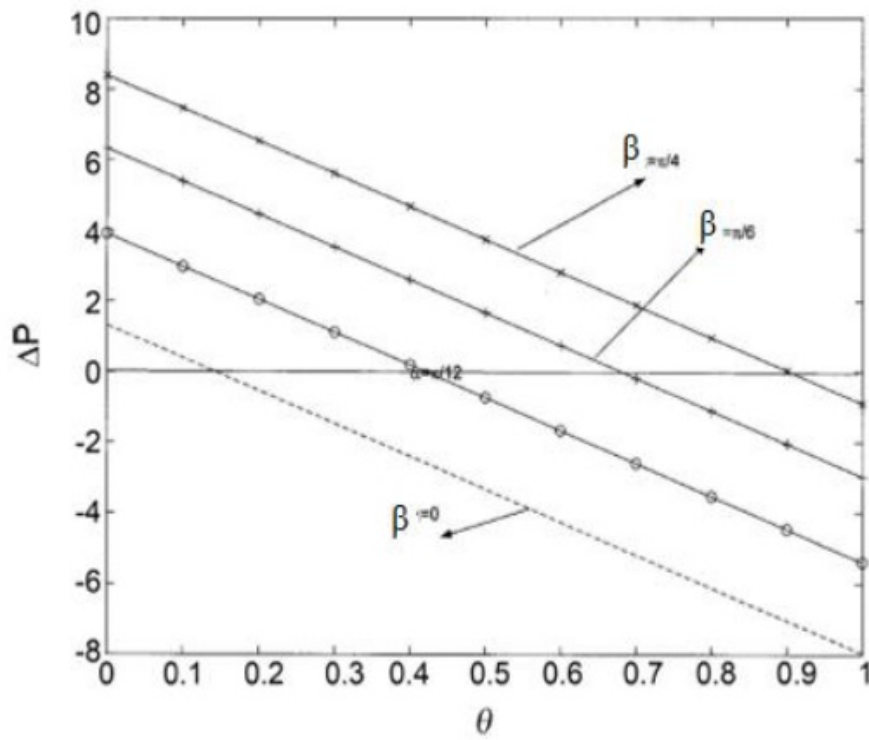


Figure 3: Variation of ΔP with θ when $F = 0.2, y_p = 0.1, \varphi = 0.3$.

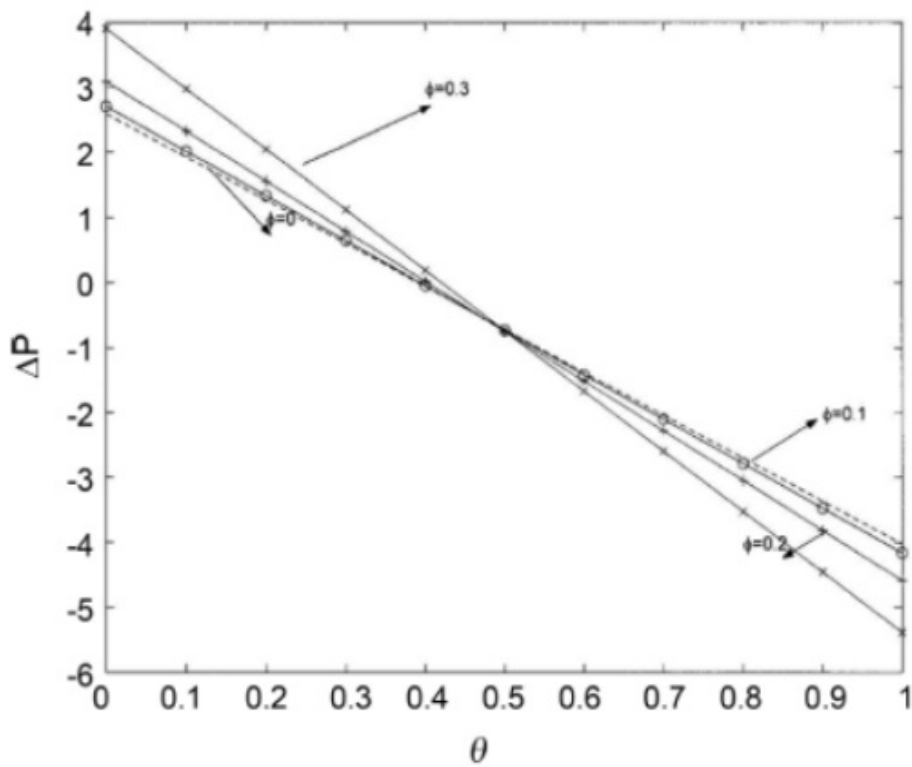


Figure 4: Variation of ΔP with θ when $F = 0.2, y_p = 0.1, \beta = \pi/10$.

in the co pumping region are crossed by a value of $\theta = 0.5$. The collective effects of angle and plug width thereby increases the area of free pumping.

The pressure increase needed to provide a zero average flow rate ΔP_0 depending on φ is seen in Figure 5. ΔP_0 increases with φ and β as well as with $\varphi \rightarrow 1$, it is found that it increases for a fixed value of β forever.

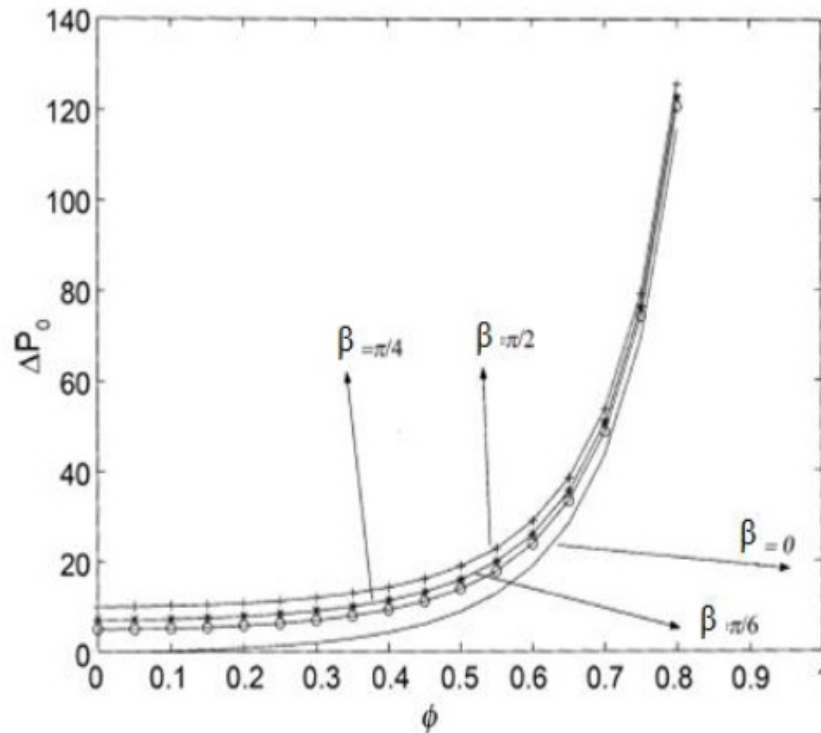


Figure 5: Variation of ΔP with φ when $F = 0.1, yp = 0.1$.

Frictional Force

In all these graphs the reverse behaviour observed with the case of ΔP , as β increases the resistance to flow, and also in fixed a as θ steadily increases the strength of friction, but ΔP reduces by θ , similar result for the variation from φ and also with yp , is found in figures 6-8. Comparable results have been obtained in the non-dimensional force $F\lambda$ versus θ , as shown in figure 6-8.

Streamlines and Fluid Trapping

The creation by closed streamlines of an inner circulating fluid bolus is called trapping, and together with the peristaltic waving is pushed this trapped bolus forward. Figures 9-11 demonstrate streamline patterns for various values of β and yp and φ using $P = 1$ and $F = 0.2$. Figure 9 illustrates the shape and fluctuation of trapped bolus at $\beta = \pi/6$ and $yp = 0.8$. The bolus is shown at different levels of φ . The trapped bolus is identified for $\varphi = 0$, but the trapping of all $f > 0$ values is noticed and the bolus size is increased by φ .

Figure 10 (where $\beta = \pi/6, \varphi = 0.4$), the bolus is not trapped at $yp \leq 0.15$ and recirculation zone creation is found at $yp = 0.3$ and the recirculating area volumes decrease and the boundary shift is noticed with the increase and extinction of $yp = 0.9$

Figure 11 illustrates several β streamline profiles with $\varphi = 0.5, yp = 0.6$. For all β . values from 0 to $\pi/2$ the production of trapped bolus is seen, with an increase in β the bolus size.

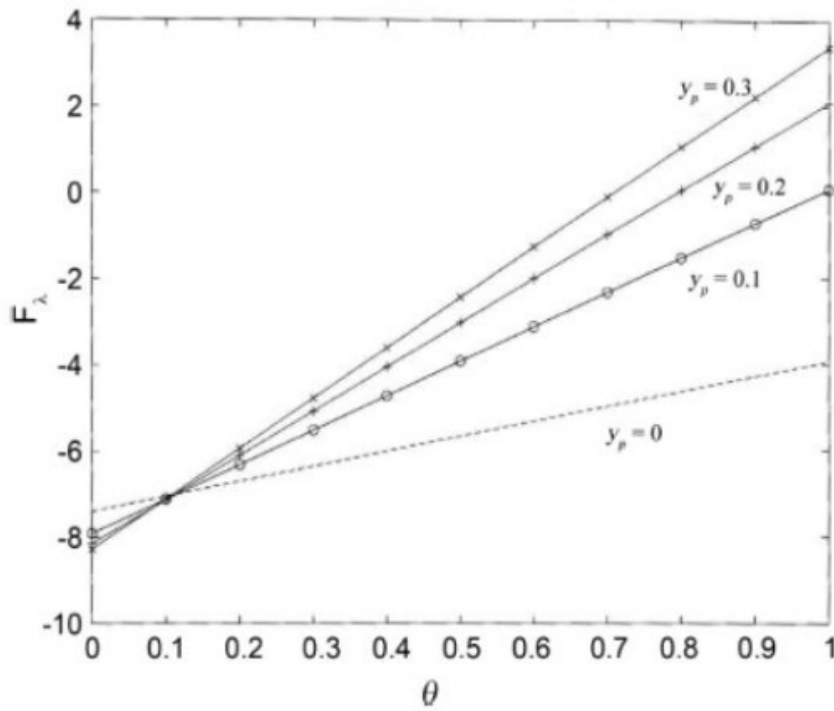


Figure 6: Variation of $F\lambda$ with θ when $F = 0.2, \beta = \pi/4, \varphi = 0.3$.

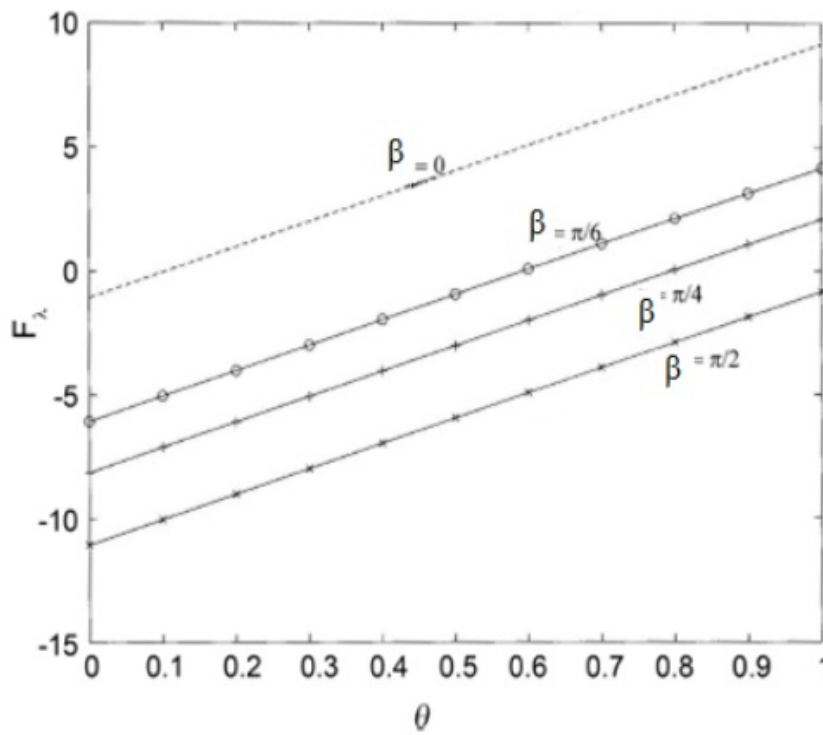


Figure 7: Variation of $F\lambda$ with θ when $F = 0.2, y_p = 0.2, \varphi = 0.3$.

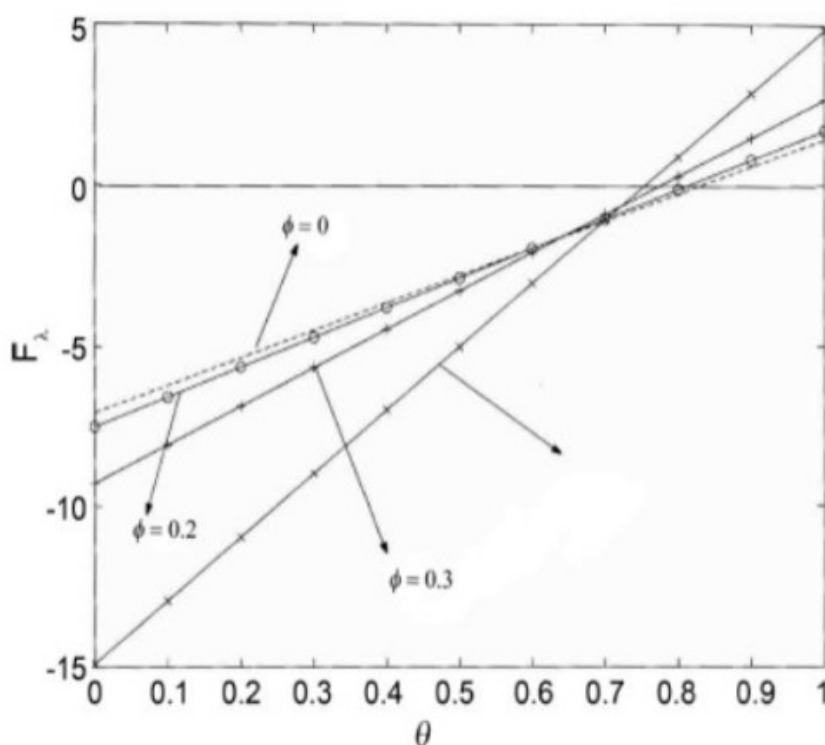


Figure 8: Variation of $F\lambda$ with θ when $F = 0.2, y_p = 0.2, \beta = \pi/4$.

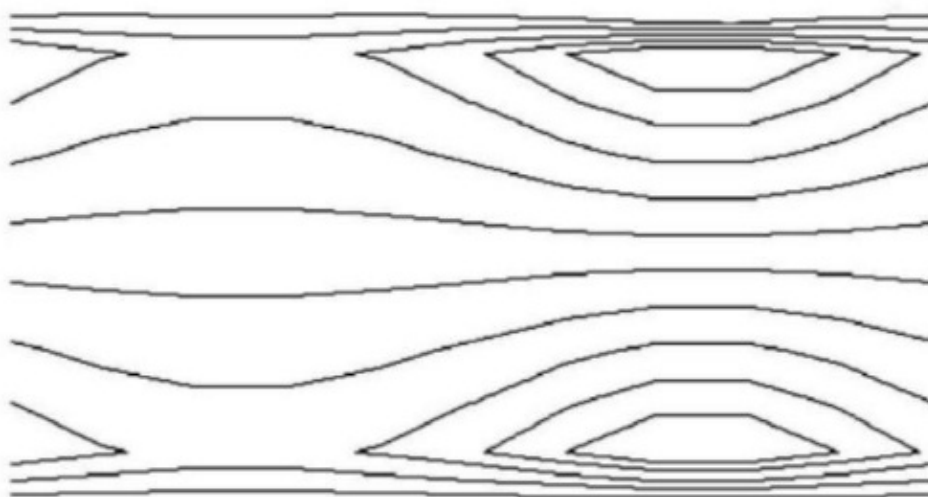


Figure 9: Streamline Profiles when $P = 1, F = 0.2, \beta = \pi/6, y_p = 0.8, \varphi = 0.8$.

6. Conclusion

The flow of the Casson fluid pipe walls is assessed according to the long wave length and low Reynolds. In a wave frame moving at wave speed, the problem is analyzed. The inclination angle and the yield stress of the fluid are noticed as the factors which have a quantitative and qualitative effect on the pressure, frictional power and forming of trapped bolus. In the existence and presence of plug width and angle of inclination, the pressure-flow curves are seen straight, with results for

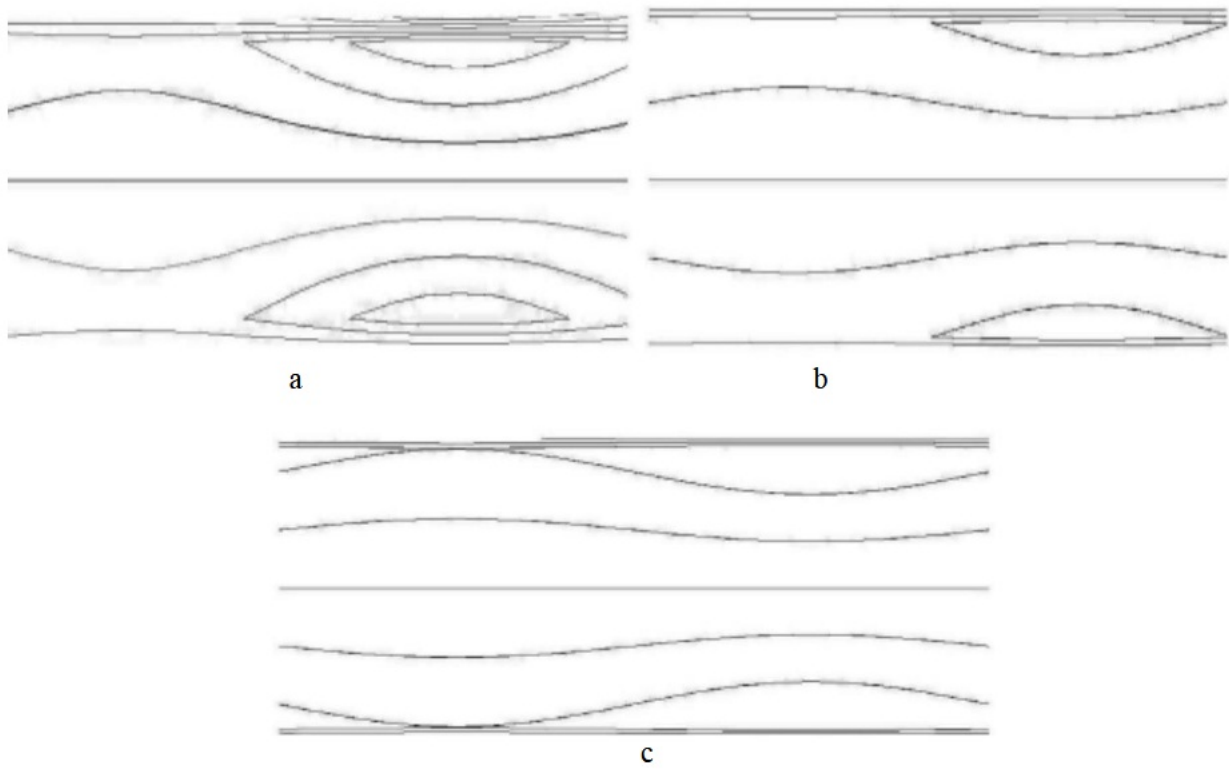


Figure 10: Streamline Profiles when $P = 1, F = 0.2, \beta = \pi/6, \varphi = 0.4$ (a) $yp = 0.3$ (b) $yp = 0.5$ (c) $yp = 0.9$.

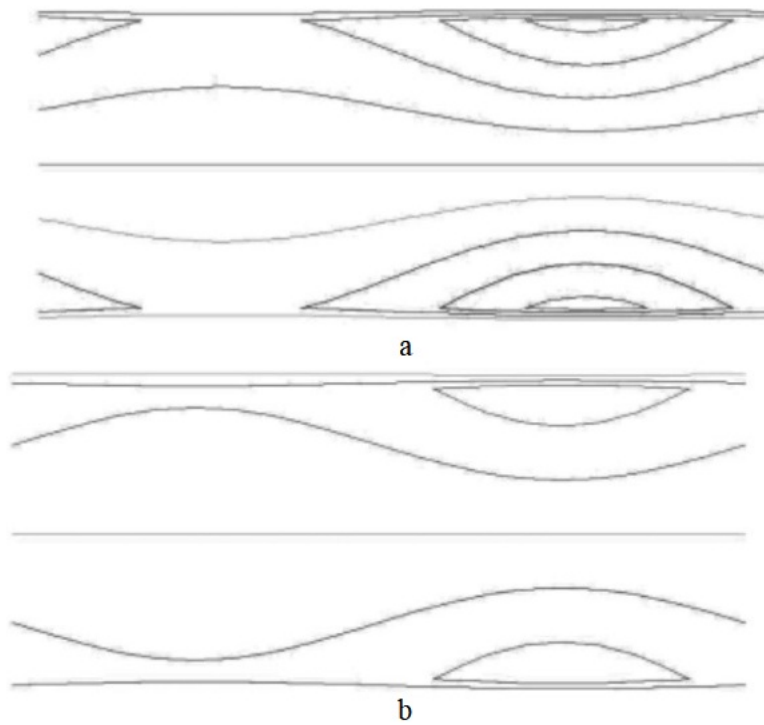


Figure 11: Streamline Profiles when $P = 1, F = 0.2, \varphi = 0.5, yp = 0.6$ (a) $\beta = \pi/6$ (b) $\beta = 0$.

adjustment of various parameters addressed. Trapping bolus creation is analyzed by changing the many parameters which occur in the issue. It is noted that the quantity of the bolus is increased and the angle and phase variation is increased and the bolus diameter reduces.

References

- [1] H. L. Agrawal and B. Anwaruddin, *Peristaltic flow of blood in a branch*, Ranchi Univ. Math. J., 15 (1984) 111-121.
- [2] N. S. Akbar, *Influence of magnetic field on peristaltic flow of a Casson fluid in an asymmetric channel: Application in crude oil refinement*, J. Magn. Mater., 378 (2015) 463-468.
- [3] M. M. Bhatti, R. Ellahi and A. Zeeshan, *Study of variable magnetic field on the peristaltic flow of Jeffrey fluid in a non-uniform rectangular duct having compliant walls*, J. Mol. Liq., 222 (2016) 101-108.
- [4] N. Casson, *Rheology of disperse systems. in Flow Equation for Pigment Oil Suspensions of the Printing Ink Type. - Rheology of Disperse Systems*, C. C. Mill, Ed., Pergamon Press, London, UK, (1959) 84-102.
- [5] P. Devaki, A. , D. V. Naidu and S. Sreenadh, *The influence of wall properties on the peristaltic pumping of a Casson fluid*, Appl. Math. Sci. Comput., (2019) 167-179.
- [6] N. Eldabe, M. Abouzeid, and H. Ali, *Effect of heat and mass transfer on Casson fluid flow between two coaxial tubes with peristalsis*, J. Adv. Res. Fluid Mech. Therm. Sci., 76 (1) 2020 54-75.
- [7] R. Ellahi, M. M. Bhatti and I. Pop, *Effects of hall and ion slip on MHD peristaltic flow of Jeffrey fluid in a non-uniform rectangular duct*, Int. J. Numer. Methods Heat Fluid Flow, 26(6) 2016 1802-1820.
- [8] P. Hariharan, V. Seshadri and R. K. Banerjee, *Peristaltic transport of Non-Newtonian fluid in a diverging tube with different waveforms*, Math. Comput. Model, 48 (2008) 998-1017.
- [9] T. Hayat, M. Javad and N. Ali, *MHD peristaltic Transport of a Jeffery Fluid in a channel with compliant walls and porous space*, Transp. Porous Med., 74 (2008) 259-274.
- [10] N. Ijaz, M. M. Bhatti and A. Zeeshan, *Heat transfer analysis in MHD flow of solid particles in non-Newtonian Ree-Eyring fluid due to peristaltic wave in a channel*, Therm. Sci., 23(2 Part B)(2017), 1017-1026 .
- [11] S. V. H. N. K. Kumari, M. V. R. Murthy, M. C. K. Reddy and Y. V. K. R. Kumar, *Peristaltic pumping of a magnetohydrodynamic Casson fluid in an inclined channel*, Adv. Appl. Sci. Res., 2 (2)(2011) 428-436.
- [12] Kh. S. Mekheimer and Y. Abd elmaboud, *The influence of heat transfer and magnetic field on peristaltic transport of a Newtonian fluid in a vertical annulus: application of an endoscope*. Phys. Lett. A, 372(2008) 1657-1665.
- [13] P. Nagarani, *Peristaltic transport of a Casson fluid in an inclined channel*, Korea-Aust. Rheol. J., 22 (2) 2010 105-111.
- [14] M. G. Reddy, K. V. Reddy and O .D. Makinde , *Heat transfer on MHD peristaltic rotating flow of a Jeffrey fluid in an asymmetric channel*. Int. J. Appl. Comput. Math., 3(4)(2017) 3201-3227 .
- [15] B.C. Sarkar, S. Das ,R. N. Jana and O.D. Makinde, *Magnetohydrodynamic peristaltic flow on nanofluids in a convectively heated vertical asymmetric channel in the presence of thermal radiation*, J. Nanofluids, 4 (2015) 1-10.
- [16] K. Vajravelu , S. Sreenadh and V. R. Babu, *Peristaltic transport of a Herschel- Bulkley fluid in an inclined tube*, Int. J. Nonlinear Mech., 40 (2005) 83-90.